J Membrane Biol (2015) 248:487–496
DOI 10.1007/s00232-015-9792-y

Phospholipid Ether Linkages Significantly Modulate the Membrane Affinity of the Antimicrobial Peptide Novicidin

Brian S. Vad[1] · Vijay S. Balakrishnan[1] · Søren Bang Nielsen[1,2] · Daniel E. Otzen[1]

Received: 16 January 2015 / Accepted: 12 March 2015 / Published online: 24 March 2015

Abstract The biological activity of antimicrobial peptides is believed to be closely linked to their ability to perturb bacterial membranes. This makes it important to understand the basis of their membrane-binding properties. Here, we present a biophysical analysis of the interactions of the antimicrobial peptide Novicidin (Nc) with ether- and ester-linked C_{14} phospholipid vesicles below and above the lipid phase transition temperature (t_p). These interactions are strongly dependent on whether the lipids contain ether or ester linkages. Nc is in random coil state in solution but undergoes a large increase in α-helicity in ether vesicles, and to a much smaller extent in ester vesicles, around the t_p. This structure is lost at higher temperatures. Steady-state fluorescence and stopped-flow kinetics using fluorophore-labeled Nc reveal that Nc binds more strongly to ether vesicles than to ester vesicles below the t_p, while there is no significant difference above the t_p. This may reflect ether lipid interdigitation in the gel phase. Isothermal titration calorimetry reveals that partitioning of Nc into both lipids is exothermic and thus enthalpy driven. The higher enthalpy associated with binding to ether lipid may be linked to Nc's higher propensity to form α-helical structure in this lipid. The large effect of the ether–ester interchange reveals that membrane–AMP interactions can be strongly modulated by charge-neutral head group changes.

✉ Daniel E. Otzen
dao@inano.au.dk

[1] Interdisciplinary Nanoscience Centre (iNANO), Center for Insoluble Protein Structures (inSPIN), Department of Molecular Biology and Genetics, Aarhus University, Gustav Wieds Vej 14, 8000 Aarhus C, Denmark

[2] Present Address: Arla Foods Ingredients Group P/S, Sønderupvej 26, 6920 Videbæk, Denmark

Keywords Antimicrobial peptide · Ether phospholipid · Ester phospholipid · Circular dichroism · Fluorescence · DSC

Introduction

Unlike conventional antibiotics, most antimicrobial peptides (AMPs) target the cell membranes (Shai 1999). AMPs bind to lipid bilayers by a combination of hydrophobic interactions with the hydrocarbon region and electrostatic/polar interactions between the charged residues of the peptide and the charged/polar lipid headgroups in the interfacial region between the water phase and the hydrocarbon region (Castanho et al. 2010). In zwitterionic bilayers, peptides like melittin and magainins (Wang 2010) assume a trans-membrane helical conformation mainly due to a hydrophobic match between the peptide length and the bilayer normal, while aureins (Seto et al. 2007) tend to remain surface-bound while still assuming a helical conformation. Most cationic peptides do not undergo a conformational change in zwitterionic ester-lipid membranes (Seto et al. 2007; Vad et al. 2010b; Balakrishnan et al. 2013) due to the absence of strong peptide–lipid electrostatic interactions. However, anionic lipids induce a significant increase in peptide α-helicity (Vad et al. 2010a; Balakrishnan et al. 2013). This is probably because the electrostatic attraction forces peptides closer to the less polar membrane environment where a helical conformation is the most favorable way of fulfilling backbone hydrogen bonding requirements (Epand and Epand 2010).

Biological membranes contain a great variety of different lipid types (O.G. Mouritsen 2005). Most are glycerophospholipids, where the fatty acid is linked to the glycerol backbone by an ester bond (O'Leary and Wilkinson 1988;

Ratledge and Wilkinson 1988; Wilkinson 1988; Mukherjee and Chattopadhyay 2005). Since AMPs are produced against eubacteria or eukaryotic microorganisms, most AMP studies naturally focus on ester-linked lipid membranes (Shai 1999; Seto et al. 2007; Vad et al. 2010a; Bertelsen et al. 2011; Dave et al. 2005; Matsuzaki et al. 1996; Nielsen and Otzen 2010; Prenner et al. 1999; Schibli et al. 2002; Zhu et al. 2006; Zhu et al. 2007). Nevertheless, ether lipids have been used as chemically more stable alternatives to ester lipids for e.g., solid-state NMR studies of AMP structures in membrane environments (Bertelsen et al. 2011; Smith et al. 1990). Furthermore, archaebacterial membrane lipids contain ether rather than ester bonds, appropriate for the harsh archaeal environments (Ratledge and Wilkinson 1988). While the polar carbonyl group is in the aqueous region of the interface in a trans-bilayer lipid profile, the ether group's lower polarity pushes the ether group lower down into the hydrophobic region (White and Wimley 1999).

Novicidin is a highly cationic antimicrobial membrane active peptide derived from sheep myeloid antimicrobial peptide, SMAP-29 (Skerlavaj et al. 1999). Nc binds to lipid membranes, and forms an α-helical structure in the presence of anionic but not zwitterionic lipids, though it permeabilizes zwitterionic membranes more efficiently than anionic membranes (Vad et al. 2010a; Balakrishnan et al. 2013; Vad et al. 2010c). In a recent study, we reported that the AMP Novicidin (Nc) assumes an α-helical structure in the presence of a zwitterionic ether lipid O-14:0-PC bicelles but not in the corresponding ester-lipid bicelles (Bertelsen et al. 2011). This implies that the ether bond can modulate AMP affinity and highlights a non-electrostatic driving force for AMP–lipid interactions. Here, we present a more detailed analysis of this phenomenon. We monitor Nc secondary structure by CD spectroscopy and by fluorescence spectroscopy using an exogenous dansyl group. Changes in the thermodynamic properties of the peptide/lipid system are monitored by calorimetry. Nc binds to both lipids, but more strongly to the ether lipid, inducing a large increase in secondary structure in the temperature region around the phase transition temperature t_p. Partitioning of Nc into either of the lipids is enthalpy driven, and the enthalpies are different only in the gel phases of the lipids, but identical in the fluid phase. We suggest that the difference in affinity is due to ether lipids' lower degree of polarity which leads to a stronger hydrophobic interaction with Nc.

Materials and Methods

DMPC (1,2-dimyristoyl-*sn*-glycero-3-phosphocholine) and O-14:0-PC (1,2-di-O-tetradecyl-*sn*-glycero-3-phosphocholine) were from avanti polar lipids (Alabaster, AL). All other reagents were from sigma aldrich. All experiments were performed in 20 mM sodium phosphate buffer pH 7.5 filtered through 0.2 μm filter. Novicidin (Nc, >98 % purity) was kindly provided by Drs. Per Holse Mygind and Hans Henrik Kristensen, Novozymes A/S. Dansyl-Nc was prepared as described (Vad et al. 2010a). Lyophilized Nc or dansyl-Nc was dissolved in the buffer and dialyzed against the same buffer twice for 1 h each and then left overnight within a membrane of MWCO 1 kDa. The concentration of Nc and dansyl-Nc were determined using molar extinction coefficients of 1280 M^{-1} cm^{-1} (Nc, 280 nm) or 4000 M^{-1} cm^{-1} (dansyl-Nc, 330 nm).

Preparation of Large Unilamellar Vesicles

The LUVs (~100 nm) were prepared as described (Vad et al. 2010a; Mayer et al. 1986) using 5 mg/ml lipid suspensions. The vesicles formed were either used immediately or kept refrigerated for use within 3–4 days. To extrude large volumes of liposomes, the barrel extruder (Northern Lipids, CA) was used, connected to a nitrogen tank at about 400 psi pressures. All extrusion was performed at least 15 °C above the t_p of the extruded lipid. Vesicle size was confirmed by dynamic light scattering (ZS Zetasizer Nano ZS, Malvern Instruments).

Circular Dichroism Spectroscopy

Far-UV (250–195 nm) wavelength scans were recorded on a Jasco 810 spectropolarimeter (Jasco Spectroscopic Co. Ltd., Hachioji City, Japan) with a 1 mm quartz cuvette (Hellmann GmbH, Germany) at 100 nm/min with a data pitch of 0.2 nm, a band width of 2 nm, response time of 1 s, and an accumulation of 6–10 spectra. For all wavelength scans, buffer/lipid spectra were subtracted from the sample spectra. Thermal scans were recorded at 220 nm from 3–100 °C at a scan speed of 90 °C/hr with a data pitch of 0.2 °C and a band width of 2 nm. CD spectra were deconvoluted to obtain the relative fractions of α-helix, β-sheet, and random coil using the program WLSQ_CD (J. S. Pedersen, unpublished).

Fluorescence Spectroscopy

Fluorescence spectra were recorded on a Varian Cary Fluorimeter (Varian, Palo Alto, CA) with a built-in peltier element for temperature regulation. 4 μM dansyl-Nc solution in a 1 cm quartz cuvette was titrated against DMPC (7.375 mM) or O-14:0-PC (6.33 mM) at different fixed temperatures between 10 and 45 °C. Lipid was added stepwise and monitored until the emission was stable, after which an emission spectrum was recorded (excitation at 335 nm, emission intensity from 400 nm to 650 nm with excitation and emission band widths of 5 nm). Binding of dansyl-Cl to lipids was measured by mixing of 4 μM

dansyl-Cl with 1.3 mM DMPC or O-14:0-PC and emission spectra were recorded (excitation at 335 nm, emission intensity from 400 to 650 nm with excitation and emission b widths of 5 nm) from 10 to 45 °C in 5 °C increments.

Differential Scanning Calorimetry

Thermograms were recorded on a VP-DSC (Microcal, Inc, Southampton, MA) instrument using 1 mg/ml lipid. Extruded LUVs with peptide and buffer solution were degassed for ~8 min at 25 °C, after which the cells were filled with the appropriate solutions, avoiding air bubbles while loading. The scans were done from 10 to 90 °C at 5 °C/h, with a data filter of 5 s. The data obtained were buffer subtracted, normalized to the lipid concentration used, and baseline corrected using cubic and linear fits options in Origin 7.0.

Stopped-Flow Measurements

Binding kinetics of dansyl-Nc to the lipid bilayers were recorded using 1:1 mixing on an applied photophysics SX-18MV reaction analyzer (Applied Photophysics, Leatherhead, Surrey) to get final concentrations of 32 μM dansyl-Nc and lipid concentrations of 1.5–600 μg/ml (~2–900 μM). The samples were excited at 335 nm and a 530 nm glass filter was used to measure the dansyl emission intensity. Time profiles (typically 20–1000 s in duration) were fitted to an appropriate number of exponential decays to obtain the amplitudes and rate constants for the associated relaxation phases.

Isothermal Titration Calorimetry

This was carried out on a VP-ITC (Microcal, Inc, Northampton, MA) instrument. To determine the enthalpy of binding of Nc to lipids, a 100 μM Nc solution was titrated in steps of 10 μl into a ~25 mM lipid solution in the calorimeter cell. Thus, lipid remained >5000-fold in excess of Nc throughout the titration. To determine Nc's lipid binding isotherm, a ~25 mM lipid solution was titrated in steps of 10 μl to a 20 μM Nc solution for O-14:0-PC and 50 μM Nc solution for DMPC at 10–45 °C. The heat of dilution for peptide into buffer was negligible. For lipid into buffer titrations, the heat of dilution was subtracted.

Results

Nc Undergoes a much Greater Conformational Change in O-14:0-PC Than in DMPC as a Function of Temperature

To follow the effect of the ether linkage lipids on the structure of Nc, we compared far-UV CD spectra of Nc in LUVs of DMPC (lipid phase transition temperature t_p 23 °C) and O-14:0-PC (t_p 27 °C), both below and above t_p (Fig. 1a, b). In the absence of lipids, Nc is largely unstructured; deconvolution of the CD spectrum suggests 68 % random coil, 24 % β-sheet, and 8 % α-helix (data not shown). At 10 °C, where both lipids exist in a gel phase (l_o), Nc maintains a state dominated by random coil, though the fraction of α-helix is now increased to around 16 % (data not shown). However, at 30 °C, where both the lipids exist in a fluid phase (l_d), the CD spectrum indicates that Nc is predominantly (~86 %) α-helical and only 13 % random coil in O-14:0-PC, while in DMPC, the distribution remains at 20 % helical and 80 % random coil (data not shown). At 45 °C, Nc is predominantly (~70 %) in the random coil state in both lipids, with the remaining 30 % equally distributed between α-helix and β-sheet. Thermal CD scans of Nc in O-14:0-PC monitored at 220 nm shows a steep increase in negative ellipticity above 23 °C, leading to a four-fold signal increase at 28 °C but returning to a level similar to the initial value around 40 °C (Fig. 1c). The corresponding signal change in DMPC was much smaller, leading to less than a doubling of the signal and confined to a much narrower temperature range (23–28 °C).

Nc Binds Strongly to O-14:0-PC

We were unable to determine the absolute affinity of Nc for the two different lipids by equilibrium dialysis experiments, centrifugation experiments, or gel filtration. This probably reflects changes to vesicle structure accompanying Nc binding such as fusion or lysis which we have previously observed (Vad et al. 2010a). These effects particularly occur at the relatively high Nc:lipid ratios required for the above-mentioned experiments. Therefore, we have to rely on more indirect means to assess binding at lower Nc:lipid ratios. We evaluated the binding of N-terminally dansyl-labeled Nc to O-14:0-PC and DMPC membranes through change in the fluorescent properties of dansyl-Nc upon transfer from water to lipid. The fluorescence intensity of dansyl-Nc increased considerably upon adding either DMPC or O-14:0-PC at 10, 20, 30, and 45 °C (Fig. 2a, b). However, the increase in intensity is consistently higher in O-14:0-PC (Fig. 2b) than in DMPC (Fig. 2a) at all temperatures, namely a factor of 2.01, 1.42, 1.185, and 1.33 at 10, 20, 30, and 45 °C respectively. This suggests either a higher binding affinity to O-14:0-PC than DMPC (a greater fraction of Nc bound) or a difference in the nature of binding. There is a marked blue-shift in λ_{max} upon addition of both lipids (Fig. 2c, d). However, the emission maximum λ_{max} is more blue-shifted in O-14:0-PC than in DMPC. In the plateau region (20-131 L:P ratios), λ_{max} is on average blue-shifted by 20, 9, 3, and 1 nm more

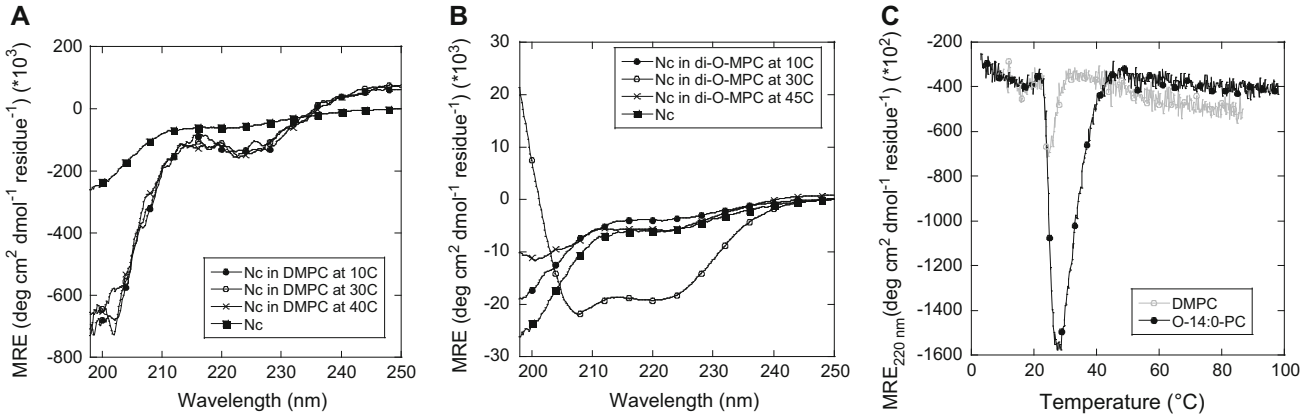

Fig. 1 Far-UV CD Spectra of Nc in **a** DMPC and **b** O-14:0-PC at 10, 30, and 45 °C. Nc is predominantly in the random coil state in all cases except in O-14:0-PC at 30 °C where it is predominantly α-helical. All spectra are recorded at a P:L molar ratio of 1:40. **c** CD thermal scans of Nc versus DMPC and O-14:0-PC at 220 nm. The ellipticity is much pronounced in O-14:0-PC compared to DMPC. Also the structure induction in O-14:0-PC around 20 °C, and its loss around 45 °C can be noticed by an increase in ellipticity. Both scans recorded at a P:L molar ratio of 1:40 and peptide concentration of 50 μM

in 0-14:0-PC than in DMPC at 10, 20, 30, and 45 °C, respectively (Table 1). This suggests greater penetration of Nc into the ether lipid, particularly below the t_m.

Binding Kinetics of Nc Differ between the Lipids in the Gel Phase

We now turn to stopped-flow techniques to investigate how greater induction of α-helicity and deeper penetration of Nc into O-14:0-PC than DMPC is reflected in the kinetics of dansyl-Nc binding to lipids. We explore the L:P range up to ca. 30 which reaches into the plateau region of λ_{max} shifts. Binding is characterized by a number of different relaxation phases, each with their own amplitude and rate constants. For simplicity, we will confine ourselves to describing the number and overall characteristics of these phases. In most but not all cases, the amplitude is negative, indicating that lipid binding is accompanied by an increase in dansyl fluorescence, consistent with Fig. 2. However, the complexity of the signals varies greatly with lipid state and lipid type.

At 10 °C where both lipids are in the gel phase, binding to DMPC only gives rise to one amplitude, which peaks around 0.6 mg/ml (Fig. 3a), and a very slow rate constant of $\sim$0.003 s^{-1} (Fig. 3a). In contrast, binding to O-14:0-PC leads to three phases, whose amplitudes increase monotonically with increasing lipid concentration (Fig. 3b) while their rate constants remain constant around 1, 0.1, and 0.01 s^{-1} (Fig. 3b). The total amplitude in the two lipids is similar. At 20 °C, which is still below the t_m, both DMPC (Fig. 3c) and O-14:0-PC (Fig. 3d) show a phase with positive amplitude, i.e., a decrease in signal. Such a decrease could be caused by a conformational change that leads to increased water exposure of the dansyl group or perhaps association with other polar lipids or peptide groups. This phase (as well as the preceding phase with negative amplitude) is around an order of magnitude faster for O-14:0-PC than for DMPC. Furthermore, O-14:0-PC has two slower phases which are absent in DMPC. At 30 °C, which is slightly above the transition temperature, both lipids have three phases (Fig. 3e, f). Although Nc forms an α-helix at this temperature in the ether lipid and not in the ester lipid (Fig. 1), there are no significant differences in rate constants. At 45 °C, the rates and amplitudes for the three relaxation phases are almost identical in the two lipids (Fig. 3g, h). Thus, the difference in binding affinity and kinetics is observed only in the gel phase of the lipids, but not in the liquid-disordered phase.

Nc Induces Thermotropic Changes in Phospholipid Membranes

DSC was employed to study how Nc affects the phase properties of the two lipid types, and hence the degree of perturbation of the lipid bilayer by the bound peptide. With increasing Nc, the t_p of both lipids shifts to lower temperatures and the transitions broaden greatly (Fig. 4). Thus, Nc heavily perturbs the bilayers of both of these lipids.

Thermodynamics of Nc Binding to DMPC and O-14:0-PC

We finally used isothermal titration calorimetry to determine the thermodynamic parameters of peptide binding and structure formation through binding isotherms. In both cases, Nc was titrated into lipid vesicles in such low

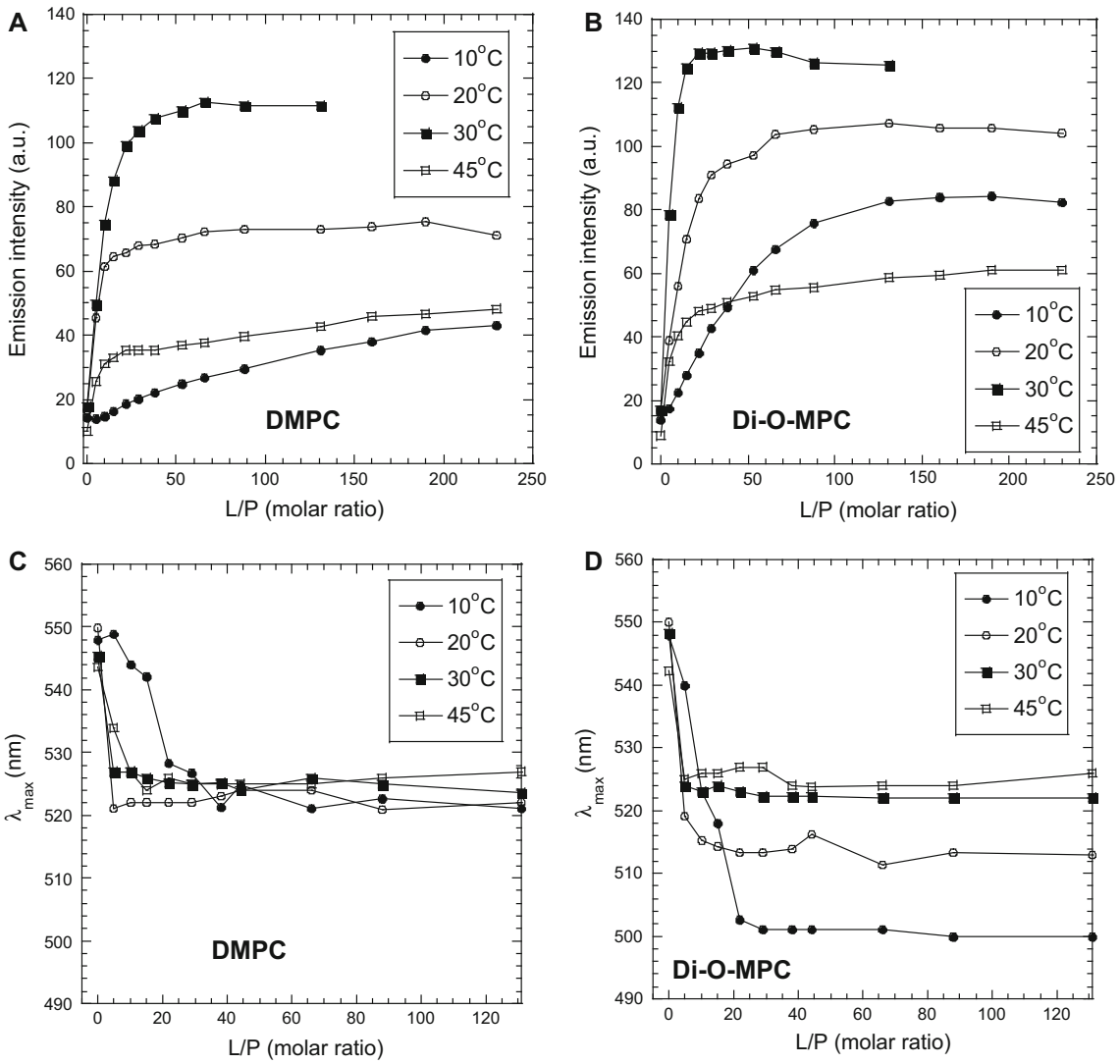

Fig. 2 Comparison of binding of dansyl-Nc to vesicles consisting of **a** DMPC and **b** O-14:0-PC measured by the emission intensity of the dansyl group. For comparison we show the shift in λ_{max} of dansyl-Nc upon binding vesicles of **c** DMPC and **d** O-14:0-PC at different temperatures as a function of L:P

Table 1 Dansyl blue-shift analysis for the binding of Nc to DMPC and O-14:0-PC at L:P = 38

Temperature (°C)	L:P = 0 (nm)[a]	L:P = 38, DMPC (nm)[a]	L:P = 38, O-14:0-PC (nm)[a]	Difference between DMPC and O-14:0-PC (nm)
10	548	521	501	20
20	550	523	514	9
30	548	525	522	3
45	542	525	524	1

[a] λ_{max} for dansyl at the indicated L:P ratios

amounts that lipids remained in great excess. This avoided possible complications from vesicle rearrangements associated with high amounts of Nc binding. In the gel phase, binding is strongly enthalpy driven for both lipids (Fig. 5a); the enthalpy value is almost three times as large for O-14:0-PC as for DMPC (Fig. 5b). In both cases, the enthalpy declines dramatically around the t_p (which is slightly higher in O-14:0-PC than in DMPC), leading to enthalpy values around zero above the t_p (Fig. 5b).

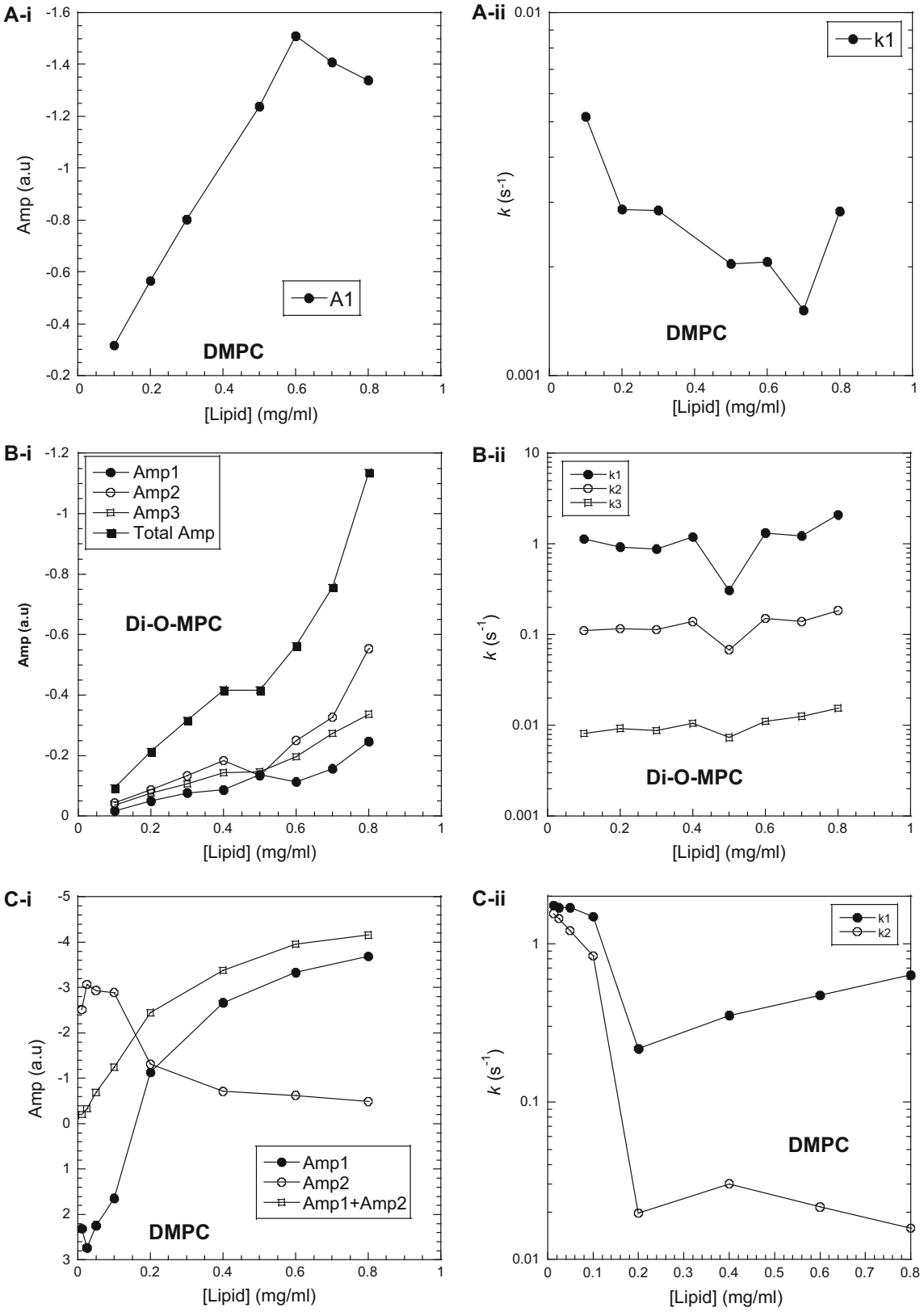

Fig. 3 Kinetics of binding of Nc to ether and ester lipids below and above the transition temperature. In each section, the amplitude A is shown in the graph with the Roman number i attached (e.g, *A-i*) and the rate constant(s) *k* obtained from the fits to the exponential decays is shown in the graph with the Roman number ii attached (e.g., *A-ii*). **a** DMPC at 10 °C. **b** O-14:0-PC at 10 °C. **c** DMPC at 20 °C. **d** O-14:0-PC at 20 °C. **e** DMPC at 30 °C. **f** O-14:0-PC at 30 °C. **g** DMPC at 45 °C. **h** O-14:0-PC at 45 °C

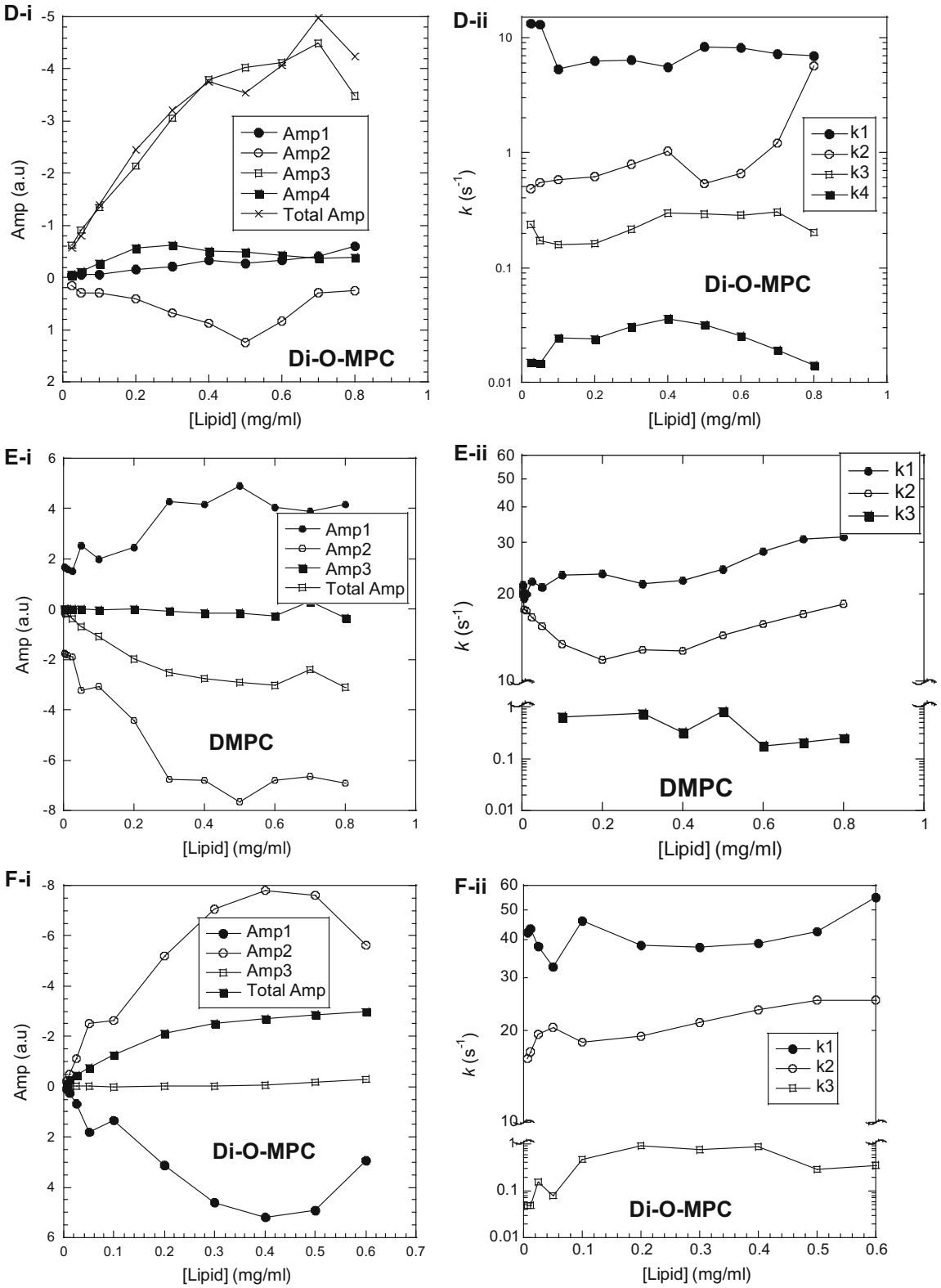

Fig. 3 continued

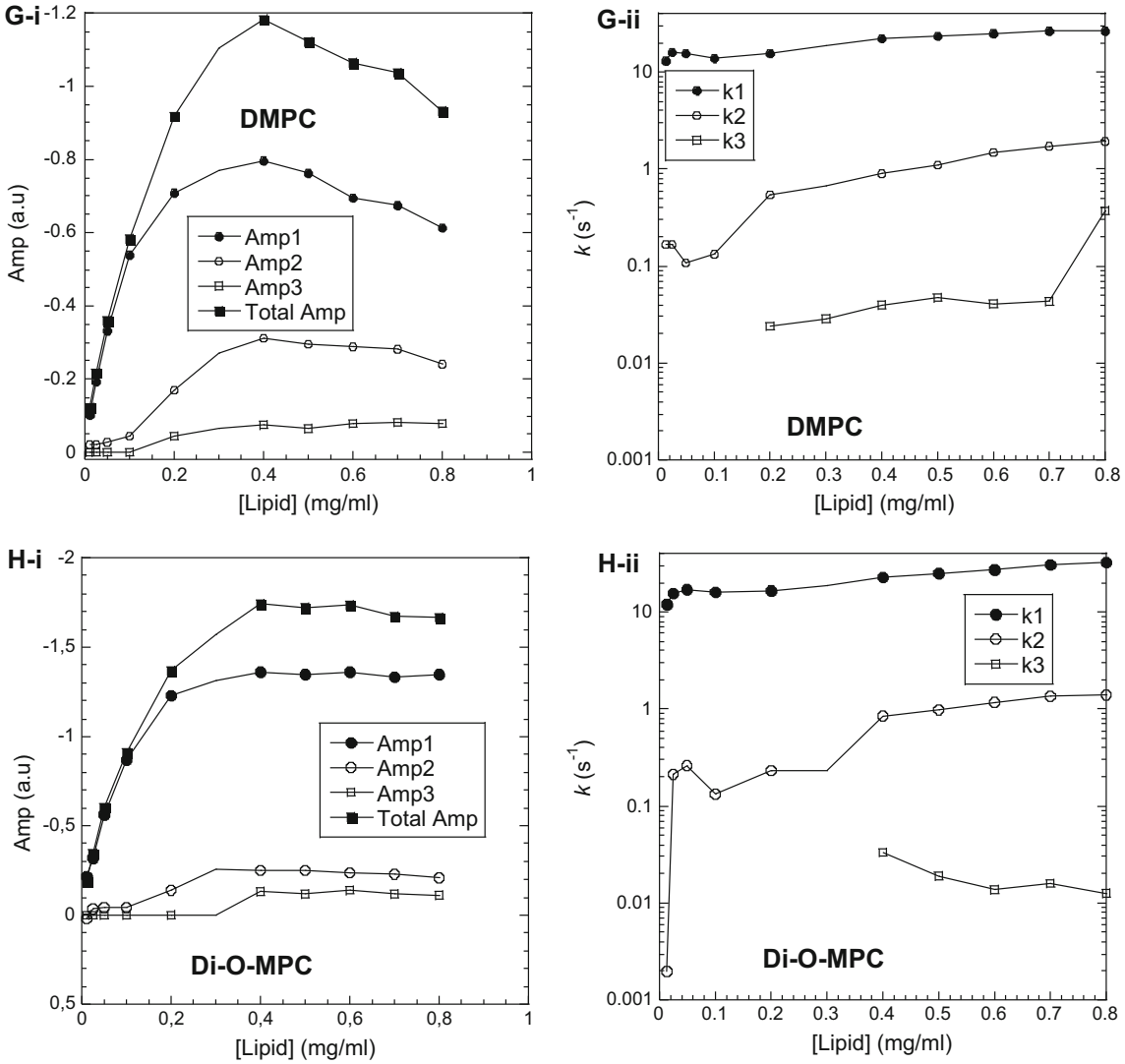

Fig. 3 continued

Discussion

Stronger Binding of Nc to Ether Lipid in the Gel Phase

Our studies on the binding of Nc to ether and ester versions of the common phospholipid DMPC show that the mode of interaction is dramatically different, particularly in the gel phase. From the CD spectra of Nc (Fig. 2) at 10 °C, it is evident that Nc is largely in the random coil state in the gel phase of both lipids but acquires a great deal of α-helical structure only in the ether lipid around its t_m, culminating at 30 °C (Fig. 3); much less structure is observed in the ester lipid. In the gel phase, Nc is clearly more deeply embedded in the ether lipid than the ester lipid, leading to a marked blue-shift in λ_{max}. The only difference between the two lipids is the less polar ether linkage in the ether lipid. We suggest that this decrease in polarity leads to a greater degree of insertion of Nc into the ether lipid in the gel phase. In the phase transition region, this greater penetration combined with increased lipid fluidity facilitates a binding mode which involves the gain of α-helical structure. However at 45 °C (Fig. 3), where both the lipids are completely melted and in a liquid-disordered phase, Nc binds with equal (low) levels of structure and degree of penetration to the two lipids. An additional factor that should be borne in mind is that in the gel phase, ether lipids but not ester lipids undergo interdigitation, i.e., they allow lipid chains from one leaflet to penetrate partially into the opposite leaflet by extending above the midplane of the bilayer (Slater and Huang 1988). This phenomenon is related to the decreased polarity of the ether lipids which drive them to reduce water exposure by submerging to a greater extent into the bilayer. The ether lipids' increased axial diffusion in the gel phase may help increased

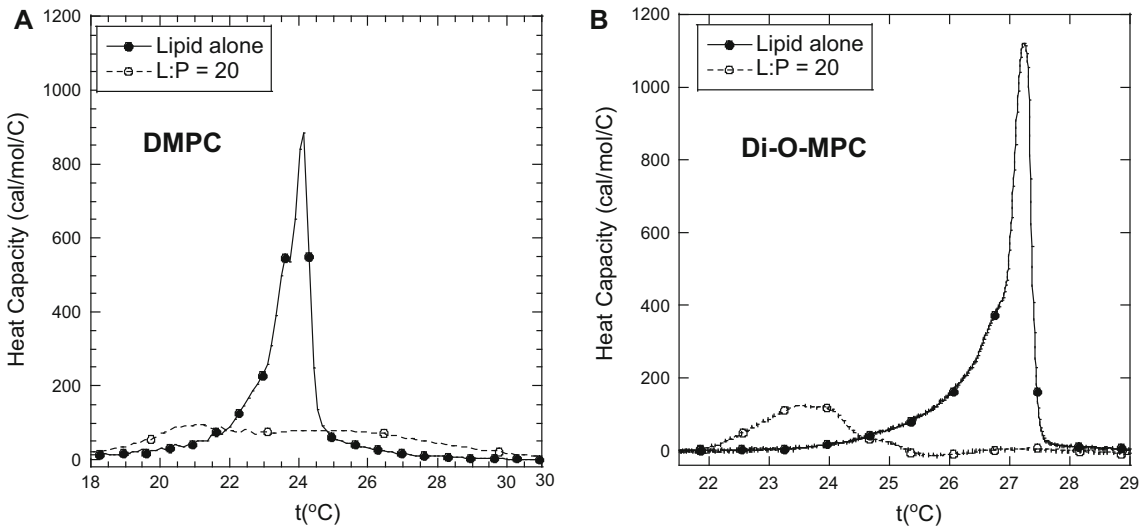

Fig. 4 Differential scanning calorimetry thermographs of Nc and vesicles made of **a** DMPC and **b** O-14:0-PC. Experiments carried out in the absence of Nc and with Nc at a L:P molar ratio of 20

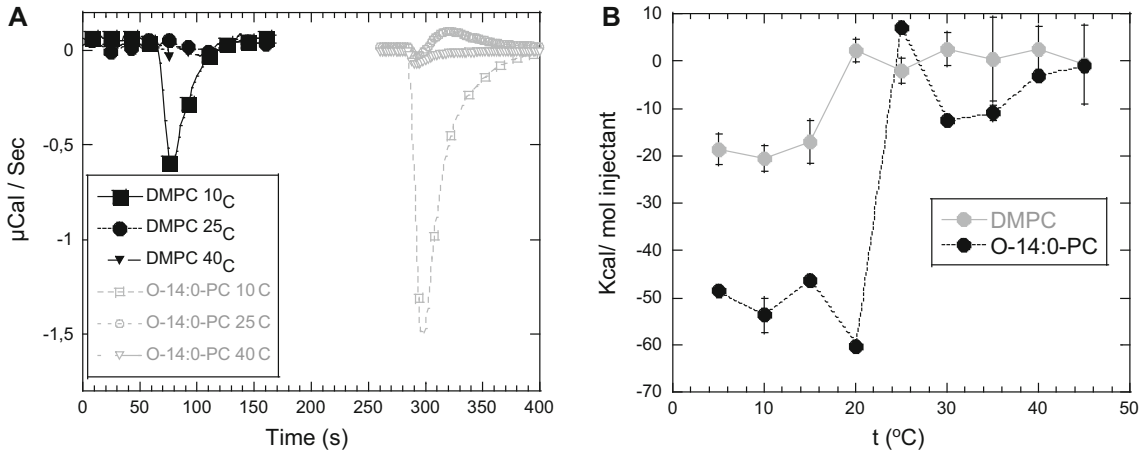

Fig. 5 Isothermal titration calorimetry experiments of the interactions between Nc and DMPC and O-14:0-PC. **a** Individual titrations into the two lipids at different temperatures. **b** Integrated enthalpies of interaction as a function of temperature

penetration of Nc into the lipid phase. In contrast, above the t_p, there is no difference in the degree of mobility of the two kinds of lipids, which tunes nicely with the observation that the mode of interaction of Nc with the lipids is very similar above the t_p (Slater and Huang 1988).

In principle, dansyl-Nc's greater blue-shift and increased intensity of signal in ether lipids could simply be ascribed to ether lipids' less polar environment (Lakowicz 2004). However, free dansyl shows the same degree of blue-shift in both lipids compared to water and report on the phase change in both lipids in a similar manner (data not shown), suggesting that the blue-shift with dansyl-Nc does not simply reflect polarity changes in the ether lipid compared to the ester lipid. Thus, the higher blue-shift for dansyl-Nc in ether lipids compared to ester lipids indicates that the N-terminus of the dansyl-Nc binds more deeply in the gel phase of the ether lipid, and this can be explained by the phenomena outlined in the previous paragraph. Similar results have been obtained for the pulmonary surfactant proteins, SP-B and SP-C (Plasencia et al. 2001). The complex and fast kinetics of binding into ether lipids further substantiate that there is a much richer scope for interactions in the ether lipid. We have previously shown (Vad et al. 2010) that Nc in fact binds in a very superficial manner to phosphocholine lipids and that binding can be enhanced by the introduction of anionic lipids (Balakrishnan et al. 2013). It is remarkable that a charge-neutral change in the lipid headgroup composition as a change from ester to ether lipids can have such profound effects on binding. This should be borne in mind when using ether

lipids rather than ester lipids as model systems for protein/peptide–lipid interactions.

Acknowledgments Brian S. Vad and Daniel E. Otzen are supported by the Danish Research Foundation (in SPIN). Vijay S. Balakrishnan is supported by the Danish Research Training Council and Novozymes A/S. We are very grateful to Anne Søndergaard and Jan Skov Pedersen for deconvoluting CD spectra using the programme WLSQ_CD.

References

Balakrishnan VS, Vad BS, Otzen DE (2013) Novicidin's membrane permeabilizing activity is driven by membrane partitioning but not by helicity: a biophysical study of the impact of lipid charge and cholesterol. Biochim Biophys Acta 1834:996–1002

Bertelsen K, Vad B, Nielsen EH, Hansen SK, Skrydstrup T, Otzen DE, Vosegaard T, Nielsen NC (2011) Long-term-stable ether-lipid vs conventional ester- lipid bicelles in oriented solid-state nmr: altered structural information in studies of antimicrobial peptides. J Phys Chem B 115:1767–1774

Castanho MARB (2010) Membrane active peptides: methods and results on structure and function. IUL Biotechnology Series, San Diego

Dave PC, Billington E, Pan YL, Straus SK (2005) Interaction of alamethicin with ether-linked phospholipid bilayers: oriented circular dichroism, 31P solid-state NMR, and differential scanning calorimetry studies. Biophys J 89:2434–2442

Epand RM, Epand RF (2010) Biophysical analysis of membrane-targeting antimicrobial peptides: membrane properties and the design of peptides specifically targeting gram-negative bacteria. Centre for Agricultural Biosciences International, Oxford

Lakowicz JR (2004) Principles of fluorescence spectroscopy, 2nd edn. Springer, New York

Matsuzaki K, Murase O, Fujii N, Miyajima K (1996) An antimicrobial peptide, magainin 2, induced rapid flip-flop of phospholipids coupled with pore formation and peptide translocation. Biochemistry 35:11361–11368

Mayer L, Hope M, Cullis P (1986) Vesicles of variable sizes produced by a rapid extrusion procedure. Biochim Biophys Acta 858:161–168

Mouritsen OG (2005) Life–as a matter of fat: the emerging science of lipidomics. Springer, Hidelberg

Mukherjee S, Chattopadhyay A (2005) Influence of ester and ether linkage in phospholipids on the environment and dynamics of the membrane interface: a wavelength-selective fluorescence approach. Langmuir 21:287–293

Nielsen SB, Otzen DE (2010) Impact of the antimicrobial peptide novicidin on membrane structure and integrity. J Colloid Interface Sci 345:248–256

O'Leary WM, Wilkinson S (1988) Microbial lipids. Academic Press, London, pp 117–202

Plasencia I, Cruz A, Casals C, Perez-Gil J (2001) Superficial disposition of the N-terminal region of the surfactant protein SP-C and the absence of specific SP-B-SP-C interactions in phospholipid bilayers. Biochem J 359:651–659

Prenner EJ, Lewis RNAH, Kondejewski LH, Hodges RS, McElhaney RN (1999) Differential scanning calorimetric study of the effect of the antimicrobial peptide gramicidin S on the thermotropic phase behavior of phosphatidylcholine, phosphatidylethanolamine and phosphatidylglycerol lipid bilayer membranes. Biochim Biophys Acta 1417:211–223

Ratledge C, Wilkinson SG (eds) (1988) An overview of microbial lipids. In: Microbial lipids, vol 1. Academic Press, London, pp 3–22

Schibli DJ, Epand RF, Vogel HJ, Epand RM (2002) Tryptophan-rich antimicrobial peptides: comparative properties and membrane interactions. Biochem Cell Biol 80:667–677

Seto GWJ, Marwaha S, Kobewka DM, Lewis RNAH, Separovic F, McElhaney RN (2007) Interactions of the Australian tree frog antimicrobial peptides aurein 1.2, citropin 1.1 and maculatin 1.1 with lipid model membranes: differential scanning calorimetric and Fourier transform infrared spectroscopic studies. Biochim Biophys Acta 1768:2787–2800

Shai Y (1999) Mechanism of the binding, insertion and destabilization of phospholipid bilayer membranes by alpha-helical antimicrobial and cell nonselective membrane-lytic peptides. Biochim Biophys Acta 1462:55–70

Skerlavaj B, Benincasa M, Risso A, Zanetti M, Gennaro R (1999) SMAP-29: a potent antibacterial and antifungal peptide from sheep leukocytes. FEBS Lett 463:58–62

Slater JL, Huang CH (1988) Interdigitated bilayer membranes. Progr Lipid Res 27:325–359

Smith R, Thomas DE, Atkins AR, Separovic F, Cornell BA (1990) Solid state 13C NMR studies of the effects of sodium ions on the gramicidin a ion channel. Biochim Biophys Acta 1026:161–166

Vad BS, Thomsen LA, Bertelsen K, Franzmann M, Pedersen JM, Nielsen SB, Vosegaard T, Valnickova Z, Skrydstrup TS, Enghild JJ, Wimmer R, Nielsen NC, Otzen DE (2010a) Divorcing folding from function: how acylation affects membrane-perturbing properties of an anti-microbial peptide. Biochim Biophys Acta 1804:806–820

Vad B, Thomsen LA, Bertelsen K, Franzmann M, Pedersen JM, Nielsen SB, Vosegaard T, Valnickova Z, Skrydstrup T, Enghild JJ (2010b) Divorcing folding from function: how acylation affects the membrane-perturbing properties of an antimicrobial peptide. Biochim Biophys Acta 1804:806–820

Vad BS, Bertelsen K, Johansen CH, Pedersen JM, Skrydstrup T, Nielsen NC, Otzen DE (2010c) Pardaxin permeabilizes vesicles more efficiently by pore formation than by disruption. Biophys J 98:576

Wang G (2010) Antimicrobial peptides: discovery design and novel therapeutic strategies. Centre for Agricultural Biosciences International, Oxford

White SH, Wimley WC (1999) Membrane protein folding and stability: physical principles. Annu Rev Biophys Biomol Struct 28:319–365

Wilkinson SG (1988) Gram-negative bacteria. In: Ratledge C, Wilkinson SG (eds) Microbial Lipids, vol 1. Academic Press, London, pp 299–488

Zhu WL, Lan H, Park IS, Kim JI, Jin HZ, Hahm KS, Shin SY (2006) Design and mechanism of action of a novel bacteria-selective antimicrobial peptide from the cell-penetrating peptide Pep-1. Biochem Biophys Res Commun 349:769–774

Zhu WL, Nan YH, Hahm K, Shin SY (2007) Cell selectivity of an antimicrobial peptide melittin diastereomer with D-amino acid in the leucine zipper sequence. J Biochem Mol Biol 40:1090–1094